AIAA JOURNAL
Vol. 46, No. 12, December 2008

Modeled Boltzmann Equation and Its Application to Shock-Capturing Simulation

R. M. C. So,* R. C. K. Leung,† and S. C. Fu‡
Hong Kong Polytechnic University, Hung Hom, 85250 Hong Kong, People's Republic of China

DOI: 10.2514/1.35332

A modified equilibrium distribution function for the Bhatnagar–Gross–Krook-type modeled Boltzmann equation has recently been proposed. The function was deduced using acoustics scaling to normalize the equation and allowed a correct recovery of similarly normalized Euler equations. It is a combination of a Maxwellian distribution plus three other terms that are moments of particle velocity. The lattice counterpart of the modified equilibrium distribution function also led to an exact recovery of the Euler equations; therefore, there is no Mach number limitation in the entire approach. This lattice counterpart was able to replicate aeroacoustics problems involving vorticity–acoustic and entropy–acoustic interactions correctly, and the simulations were carried out using a finite difference lattice Boltzmann method employing only a two-dimensional, nine-velocity lattice. Thus formulated, the numerical scheme has no arbitrary constants and all calculations were carried out using one single relaxation time and a set of constants derived from the analysis. This paper investigates the validity and extent of the formulation to capture shocks and resolve contact discontinuity and expansion waves in one- and two-dimensional Riemann problems. The simulations are carried out using the same two-dimensional, nine-velocity lattice, and identical set of constants and relaxation time; they are compared with theoretical results and those obtained by solving the Euler equations directly using Harten's first-order numerical scheme. Good agreement is obtained for all test cases. However, the modified equilibrium distribution function is not suitable for shock structure simulation; for that, an exact recovery of the Navier–Stokes equations is required.

I. Introduction

AN ATTEMPT to simulate shock waves using the Boltzmann equation (BE) has been made by Mott-Smith [1] who proposed a bimodal distribution function consisting of two Maxwellian terms to describe molecular collision behavior in the BE. The solution was then compared with an approximate solution of the BE for strong shocks where the Chapman–Enskog [2] expansion method was used to recover the Navier–Stokes (NS) equations. This approach proved to be satisfactory for the simulation of the structure of strong shocks but was not valid for shocks with low to moderate Mach numbers M. Extension of the Mott-Smith approach to low to moderate M was attempted by Salwen et al. [3]. Since then, attempts to model the BE have been made by various researchers; among them, a commonly accepted model was that due to Bhatnagar et al. [4], hereafter designated as the BGK model. The model was proposed for monatomic gas only and considered the deviation of the particle distribution function f from its equilibrium state f^{eq} to be small. Thus, the nonlinear character of molecular collision was modeled in f^{eq}, which BGK assumed to be described by a Maxwellian distribution. The lattice Boltzmann method (LBM) devised from this model found success in the simulation of incompressible, isothermal flow, where the equation of state for monatomic gas is automatically satisfied. Its extension to simulate compressible air flows, even with low Mach number ($M < 0.3$), was not satisfactory, and the specific heat ratio for a diatomic gas was not recovered correctly [5].

Since then, various attempts have been made to remedy the shortcomings of the BGK model. A lattice Boltzmann simulation scheme was introduced to model thermodynamic flows of monatomic gas [6] while higher-order velocity expansion for f^{eq} was used to recover macroscopic equations without the nonlinear deviation terms [7]. Attempts to simulate compressible flows with moderate to relatively high M using a BGK-type modeled BE have been made by numerous researchers. Their attempts can be broadly classified into two different approaches. One approach aimed to recover the Euler equations only to resolve shocks, contact discontinuity, and expansion waves in the flow [8–10]. This same classification can also include those studies that proposed to recover the NS equations, but the actual interest was aimed at shock capturing [11–16]. Another approach attempted to simulate shock structures by solving the modeled BE and/or at least recover the NS equation [17–20], albeit subject to limitation on M.

The approach adopted to recover the compressible Euler equations was based on the BGK model [8–10]; however, the recovery was not accomplished by modifying the continuous f^{eq}, rather it was achieved through an assumption for a lattice equivalent of f^{eq}. To make the lattice Boltzmann method, based on the assumed lattice form of f^{eq}, applicable to diatomic gas, the equation of state was invoked by relating the pressure p to the gas density ρ and the internal energy e. Thus, the specific heat ratio γ was specified as 1.4 for diatomic gas [8–10]. In the study by Yan et al. [8], good agreement with other numerical results was achieved by adopting a two-dimensional, 17-velocity lattice model (D2Q17). One drawback of this approach is that there are many free parameters and the comparison with Roe's test [9] is not as good. On the other hand, a finite difference lattice Boltzmann model (FDLBM) possessing both kinetic and thermal energies was proposed by Shi et al. [9]. Their approach was able to remedy some of the shortcomings of the Yan et al. [8] approach, even using a two-dimensional, nine-velocity (D2Q9) lattice model for the simulation of 1-D Riemann problems. However, they had to adopt a total variation diminishing (TVD) scheme to suppress numerical oscillations resulting from their simulations. Another model using a small number of discrete velocities was proposed by Kataoka and Tsutahara [10] but with a different lattice f^{eq} assumed. With this modified lattice f^{eq}, they demonstrated that the calculated macroscopic variables were able to

Received 27 October 2007; accepted for publication 23 July 2008.

*Professor Emeritus, Department of Mechanical Engineering, also the Industrial Center; mmmcso@polyu.edu.hk. Fellow AIAA (Corresponding Author).

†Assistant Professor, Department of Mechanical Engineering. Senior Member AIAA.

‡Research Assistant, Department of Mechanical Engineering.

exactly satisfy the compressible Euler equations with flexible specific heat ratio γ in the limit of small Knudsen number Kn. Sun [11] attempted to solve the BE using an adaptive LBM. Extension to 3-D compressible flows with shocks has also been carried out [12]. All of these proposals have one thing in common: they could not be easily generalized to 3-D flows because there is no formal methodology to follow to allow a 3-D equivalent lattice f^{eq} to be proposed and/or formulated.

Extension of the preceding approach to recover the NS equations could also be a concern. Consequently, a straightforward extension of a lattice BGK to recover the NS equations leads to an additional nonlinear deviation term on the right-hand side of the momentum equation [7]. Another difficulty was the exact recovery of the compressible NS equations with a flexible specific heat ratio γ. Tsutahara et al. [15] proposed the use of one additional distribution function to simulate the internal degree of freedom and an FDLBM scheme was used to solve the resulting equation. Their approach was based on a lattice f^{eq} where expansions in terms of the temperature T and velocity u_i were assumed [16]. However, the form of the lattice f^{eq} was given with little or no details provided on how this form was obtained. The model was able to replicate 1-D Riemann problems with results comparable to those given by solving the compressible NS equations using the MacCormack method [21].

Simulation of shock structure in high Mach number flows ($M > 2$) has also been attempted [1,17–20]. A bimodal distribution proposed by Mott-Smith [1], which was substantially different from the conventionally assumed Maxwellian distribution [2], was found suitable for high Mach numbers and strong shock structure simulation. As pointed out by Salwen et al. [3], the polynomial expansion of f^{eq} could not handle strong shocks, that is, it could only simulate flows with $M < 2$. One drawback of Mott-Smith's proposal [1] is that it cannot recover the NS equations for weak shocks ($M \sim 1$). Salwen et al. [3] extended the proposal by adding some "correction terms" to bring the Mott-Smith [1] method into agreement with aerodynamic theories for weak shocks. For the framework under the BGK model, Qian and Orszag [17] reported and investigated the nonlinear deviation from the NS equations for shock structures. Other simulations [18,19] were based on the two reduced-functions method of Chu [20]. In these simulations, two distribution functions that are the moment integrals of f were introduced. The integrations were performed over the entire velocity space. A discrete ordinate method was used to solve the governing equations by first removing the velocity space dependency from the distribution functions so that the modeled BE could be solved in the phase space [18,19]. Compressible 1-D and 2-D flows with $M \leq 12$ have been attempted, and good agreement with direct Monte Carlo simulation results of the same problems was obtained. A third approach was to solve the BE using an adaptive LBM [12] and its extension to 3-D flows with shocks [13].

Instead of the LBM, FDLBM, and discrete ordinate method, another approach based on the BGK model is the gas-kinetic scheme for compressible flows [22–27]. Initially, the attempt was made to use this scheme to recover the compressible Euler equations [22] and then applied it to solve certain benchmark 1-D shock problems. Extension to solve 2-D wedge and ramp problems at higher M was subsequently made [23]. The scheme was extended to recover the NS equations and simulate flows with low M [24,25]. Extension of the viscous approach to simulate high M flows and the resolution of shock structures was also carried out [26,27]. This scheme was based on a multidimensional gas evolution model. The rationale was that a nonequilibrium state would evolve into an equilibrium state along the direction of increasing entropy. The scheme was verified to return to two numerical limits, a one-step Lax–Wendroff scheme and a kinetic flux vector splitting scheme.

Yet another approach to model the BE has been put forward by Fu et al. [28]. Their original aim was to use the modeled BE to simulate aeroacoustics problems; therefore, they started with acoustics scaling [29] to normalize the variables and the modeled BE. To recover the Euler equations correctly from the BGK-type modeled BE, they made the exact recovery of the Euler equations a requirement and then proceeded to find the conditions under which this requirement could be satisfied. This led to a modified equilibrium distribution function (MEDF; hereafter, f^{eq} is used to denote this MEDF) that is made up of the traditional Maxwellian distribution plus three more terms that are first and second moments of f, and an additional equation of the Poisson type for a second-order tensor that needs to be solved simultaneously with the modeled BE. In addition, the internal energy definition was modified to include the effect of particle rotation, so that the approach is applicable to both monatomic and diatomic gases. This ensured that $\gamma = 1.4$ for the state equation of diatomic gas is recovered identically. They solved the modeled BE using a sixth-order accurate FDLBM, thus necessitating the need to derive a lattice counterpart for f^{eq} such that the Euler equations can also be recovered correctly from the discrete approach. Consequently, their formulation is not subject to any M limitation. The FDLBM was solved using a D2Q9 lattice model and the solutions were validated against benchmark aeroacoustics problems that involved vorticity–acoustic and entropy–acoustic interactions. Very good agreement with analytical and direct numerical simulation solutions of the same problems was obtained.

Einstein once said "Everything should be made as simple as possible, but not simpler." It is in this spirit that an attempt is made to extend the BGK-type modeled BE without further modifications to capture shocks in compressible flows, because the formulation of Fu et al. [28] is for inviscid flows only. Derivation details of the continuous f^{eq} and its lattice counterpart are available in Fu et al. [28], and are not repeated here. However, for the sake of completeness, a brief description of the modified BGK-type modeled BE and its lattice counterpart is given here.

II. Bhatnagar–Gross–Krook-type Modeled Boltzmann Equation

The basis of the present method is the BGK-type modeled BE which is given by

$$\frac{\partial \hat{f}}{\partial \hat{t}} + \hat{\boldsymbol{\xi}} \cdot \nabla_{\hat{x}} \hat{f} = -\frac{1}{\hat{\tau}} (\hat{f} - \hat{f}^{\text{eq}}) \tag{1}$$

where $\hat{\boldsymbol{\xi}}$ is the particle velocity vector, $\hat{t}$ is time, $\hat{\boldsymbol{x}}$ is the position vector (from this point on, boldface and indices are used interchangeably to denote vectors), $\hat{\tau}$ is the particle collision relaxation time, and the "hat" is used to denote dimensional quantities. The corresponding dimensionless variables are denoted by the same symbols without the hat. The acoustics scaling form of the Euler equations [29] are obtained by choosing the reference sound speed $\hat{c}_r$ as the characteristic velocity for both $\hat{u}_i$ and $\hat{\boldsymbol{\xi}}$, $\hat{L} = \hat{x}_o / Kn$ as the characteristic length, the mesoscopic time $\hat{\tau}_o$ as the characteristic time, the reference density $\hat{\rho}_r$ as the characteristic density, $\hat{c}_r^2 / \hat{C}_{pr}$ as the characteristic temperature, $\hat{\rho}_r \hat{c}_r^2$ as the characteristic pressure, and $\hat{\rho}_r / \hat{c}_r^D$ as the characteristic scale for $\hat{f}$ and $\hat{f}^{\text{eq}}$. If $\theta = (R/\hat{C}_{pr})T$ is defined, then the equation of state is given by $p = \rho\theta$ where p is pressure. The Knudsen number $Kn = \hat{x}_o / \hat{L}$ is dimensionless, R is the universal gas constant and is dimensional, $\hat{x}_o$ is the mesoscopic length, $\hat{C}_{pr}$ is the reference specific heat at constant pressure, and D is the dimension of the problem (2 for 2-D and 3 for 3-D flow).

An MEDF to replace the Maxwellian distribution conventionally assumed in the BGK-type model is sought. This f^{eq} is required to satisfy the macroscopic constraints such that the recovered macroscopic transport equations are exactly valid for diatomic gas and are not subject to the $M \ll 1$ assumption.

The macroscopic continuum transport equations (i.e., $Kn \ll 1$) can be derived from a Chapman–Enskog [2] expansion of Eq. (1) in terms of Kn. The expansions for the dependent and independent variables and their derivatives can be written as

$$x_i = x_i^{(1)} + Kn x_i^{(2)} + \mathcal{O}(Kn^2) \tag{2a}$$

$$t = t^{(1)} + Kn t^{(2)} + \mathcal{O}(Kn^2) \tag{2b}$$

$$f = f^{(0)} + Knf^{(1)} + Kn^2 f^{(2)} + \mathcal{O}(Kn^3) \tag{2c}$$

$$\frac{\partial}{\partial t} = \frac{\partial}{\partial t^{(1)}} + Kn\frac{\partial}{\partial t^{(2)}} \tag{2d}$$

$$\frac{\partial}{\partial x_i} = \frac{\partial}{\partial x_i^{(1)}} \tag{2e}$$

Collecting terms of the same Kn order gives rise to a set of equations for $f^{(n)}$. The zero-order solution for f is simply $f^{(0)} = f^{\mathrm{eq}}$, whereas the first-order equation is given by

$$\frac{\partial f^{(0)}}{\partial t^{(1)}} + \boldsymbol{\xi}\cdot\nabla_{x^{(1)}} f^{(0)} = -\frac{f^{(1)}}{\tau}, \qquad \text{to } \mathcal{O}(Kn) \tag{3}$$

Because only $f^{(1)}$ is required for the recovery of the Euler equations [28], solution for $f^{(2)}$ is not necessary. All integrals of higher-order terms $f^{(n)}$ and their moments are required to be zero for $n \geq 1$ [30]. It is obvious that $f^{(0)}$ and $f^{(1)}$ are related to f^{eq}, therefore, it is necessary to construct an f^{eq} that satisfies the macroscopic constraints if the Euler equations were to be recovered exactly.

The macroscopic constraints are γ, ρ, $\rho\boldsymbol{u}$ and e. For the derived results to be applicable to diatomic gas, both the translational degree of freedom D_T and the rotational degree of freedom D_R of particle motions are considered in the energy model for e. Therefore, the constraints are given by

$$\rho = \int f^{\mathrm{eq}}\,\mathrm{d}\boldsymbol{\xi} \tag{4a}$$

$$\rho u_i = \int f^{\mathrm{eq}}\xi_i\,\mathrm{d}\boldsymbol{\xi} \tag{4b}$$

$$\rho e + \frac{1}{2}\rho|\boldsymbol{u}|^2 = \frac{D_T + D_R}{D}\int\frac{1}{2}f^{\mathrm{eq}}|\boldsymbol{\xi}|^2\,\mathrm{d}\boldsymbol{\xi} = \int\frac{1}{2}f^{\mathrm{eq}}|\boldsymbol{\xi}-\boldsymbol{u}|^2\,\mathrm{d}\boldsymbol{\xi} + \frac{K}{D}\int\frac{1}{2}f^{\mathrm{eq}}|\boldsymbol{\xi}|^2\,\mathrm{d}\boldsymbol{\xi} + \frac{1}{2}\rho|\boldsymbol{u}|^2 \tag{4c}$$

with the stipulation that higher-order terms $f^{(n)}$ and their moments have to satisfy the following conditions [30]:

$$\int f^{(n)}\,\mathrm{d}\boldsymbol{\xi} = 0 \quad \text{for all } n \geq 1 \tag{5a}$$

$$\int f^{(n)}\boldsymbol{\xi}\,\mathrm{d}\boldsymbol{\xi} = 0 \quad \text{for all } n \geq 1 \tag{5b}$$

$$\frac{D_T + D_R}{D}\int\frac{1}{2}f^{(n)}|\boldsymbol{\xi}|^2\,\mathrm{d}\boldsymbol{\xi} = 0 \quad \text{for all } n \geq 1 \tag{5c}$$

In Eq. (4c), $(\boldsymbol{\xi}-\boldsymbol{u})$ is the peculiar velocity of a particle, D is the problem dimension, $K = D_T + D_R - D$ is the number of internal degrees of freedom, and the integral is evaluated over the entire velocity space. This energy model is different from that assumed in the original BGK model. Fu et al. [28] have shown that the second term in Eq. (4c) is sufficient to allow γ for a diatomic gas to be correctly recovered. Hence, $e = \theta/(\gamma-1)$, which is a consequence of the equipartition theorem, and the speed of sound c is given by $c^2 = \gamma\theta$, where $\gamma = (D_T + D_R + 2)/(D_T + D_R)$. For diatomic gas, $D_T = 3$ and $D_R = 2$, thus yielding $\gamma = 1.4$ exactly, and a correct c and e.

The continuity equation can be recovered exactly from the integral of Eq. (3) with respect to $\mathrm{d}\boldsymbol{\xi}$ by first setting $f^{(0)} = f^{\mathrm{eq}}$, whereas the momentum equation can be derived from the integral of Eq. (3) by first multiplying it by ξ_i to give

$$\int\left[\frac{\partial f^{\mathrm{eq}}}{\partial t} + \frac{\partial}{\partial x_j}(\xi_j f^{\mathrm{eq}}) = -\frac{f^{(1)}}{\tau}\right]\xi_i\,\mathrm{d}\boldsymbol{\xi} \Rightarrow \frac{\partial(\rho u_i)}{\partial t} + \frac{\partial}{\partial x_j}(P_{ij} + \rho u_i u_j) = 0 \tag{6}$$

where all $t^{(1)}$, $x_j^{(1)}$, and $f^{(1)}$ have been replaced by t, x_j, and f from this point on. The energy equation can be obtained from the integral of Eq. (3) by first multiplying it by $(|\boldsymbol{\xi}|^2/2)[(D_T + D_R)/D]$ to give

$$\begin{aligned}
&\int\left[\frac{\partial f^{\mathrm{eq}}}{\partial t} + \frac{\partial}{\partial x_j}(\xi_j f^{\mathrm{eq}}) = -\frac{f^{(1)}}{\tau}\right]\frac{|\boldsymbol{\xi}|^2}{2}\left(\frac{D_T + D_R}{D}\right)\mathrm{d}\boldsymbol{\xi}\\
&\quad\Rightarrow \frac{\partial}{\partial t}\left(\rho e + \frac{1}{2}\rho|\boldsymbol{u}|^2\right) + \frac{D_T + D_R}{D}\frac{\partial}{\partial x_j}\left\{Q_j + u_j\left(\frac{1}{2}\rho|\boldsymbol{u}|^2 + \frac{1}{2}P_{kk}\right) + u_k P_{jk}\right\} = 0\\
&\Rightarrow \frac{\partial}{\partial t}\left(\rho e + \frac{1}{2}\rho|\boldsymbol{u}|^2\right) + \frac{\partial}{\partial x_j}\left[u_j\left(\rho e + p + \frac{1}{2}\rho|\boldsymbol{u}|^2\right)\right]\\
&\quad + \frac{\partial}{\partial x_j}\left[\frac{D_T + D_R}{D}Q_j + \frac{D_T + D_R - D}{D}u_j\left(\frac{1}{2}\rho|\boldsymbol{u}|^2\right) + \frac{D_T + D_R - D}{D}pu_j + \frac{D_T + D_R}{D}\frac{1}{2}u_j P'_{kk}\right.\\
&\quad\left. + \frac{D_T + D_R}{D}u_k P'_{jk}\right] = 0\\
&\Rightarrow \frac{\partial}{\partial t}\left(\rho e + \frac{1}{2}\rho|\boldsymbol{u}|^2\right) + \frac{\partial}{\partial x_j}\left[u_j\left(\rho e + p + \frac{1}{2}\rho|\boldsymbol{u}|^2\right)\right] + \frac{\partial}{\partial x_j}(Q'_j) = 0
\end{aligned} \tag{7}$$

In deriving Eqs. (6) and (7), the following expressions

$$\int(\xi_i)(\xi_j)f^{\mathrm{eq}}\,\mathrm{d}\boldsymbol{\xi} = P_{ij} + \rho u_i u_j = p\delta_{ij} + P'_{ij} + \rho u_i u_j \tag{8a}$$

$$\frac{1}{2}\int(\xi_j)|\boldsymbol{\xi}|^2 f^{\mathrm{eq}}\,\mathrm{d}\boldsymbol{\xi} = Q_j + u_j\left(\frac{1}{2}\rho|\boldsymbol{u}|^2 + \frac{1}{2}P_{kk}\right) + u_k P_{jk} \tag{8b}$$

have been assumed after using the constraints given in Eqs. (4) and (5). If the momentum and the energy equations were to be recovered identically for an inviscid fluid, then

$$\partial P'_{ij}/\partial x_j = 0 \quad \text{and} \quad \partial Q'_j/\partial x_j = 0 \tag{9}$$

have to be satisfied. The second condition in Eq. (9) could be replaced by a stronger one, that is, $Q'_j = 0$ with no loss of generality [28]. Thus, the correct recovery of the Euler equations hinges on a known f^{eq} and an appropriate construction of P'_{ij}.

The expression for P'_{ij} [Eq. (8a)] leads to a definite value for P'_{ii}, but the individual elements of P'_{ij} still need to be evaluated. This can be accomplished once f^{eq} is known. For monatomic gas, f^{eq} is given by the Maxwellian distribution function alone [31]. The objective here is to find an MEDF (f^{eq}) for diatomic gas that could satisfy the constraints given by ρ, $\rho\boldsymbol{u}$, e, P'_{ij}, and Q_j [Eqs. (4) and (5)]. To determine f^{eq} and P'_{ij}, Fu et al. [28] adopted an approach that made use of a known f^{eq} to solve for P'_{ij}. The known f^{eq} was deduced with guidance from previous analytical work [32–34] and is given by

$$f^{\mathrm{eq}} = \alpha_0 \exp\left[-\eta \sum_{k=1}^{D} (\xi_k - b_k)^2\right] + \sum_{i=1}^{D} \alpha_i \xi_i \exp[-\eta|\boldsymbol{\xi}|^2] + \sum_{m,n=1}^{D} \beta_{mn}\xi_m\xi_n \exp[-\eta|\boldsymbol{\xi}|^2] + \sum_{j=1}^{D} a_j \xi_j |\boldsymbol{\xi}|^2 \exp[-\eta|\boldsymbol{\xi}|^2] \quad (10)$$

where α_0 is a scalar, α_j, a_j, and b_i are vectors, β_{mn} is a second-order tensor, and η is a parameter to be determined. The first term on the right-hand side of Eq. (10) is the Maxwellian distribution term, whereas the other three terms are the first and second moments of the particle velocity. These additional terms attempt to model the nonlinear behavior resulting from particle–particle collisions. Equation (10) differs from conventionally known forms of f^{eq} used and/or proposed by other researchers. The presence of the additional three terms in Eq. (10) is sufficient to allow aeroacoustic disturbances to be resolved accurately [28]. In other words, the proposed modeling of particle–particle collisions in Eq. (10) could correctly account for the effect of aerodynamic and acoustic interaction [28]. It remains to be seen whether this same f^{eq} is suitable for resolving shocks, contact discontinuity, and expansion waves in compressible flows at any M.

The constraints given by Eqs. (4), (5), and (8a) plus the assumption $Q'_j = 0$ lead to the following equations for $\alpha_0, \alpha_j, a_j, b_i$, and β_{mn}, that is,

$$\rho = \left(\alpha_0 + \sum_{m}^{D} \frac{\beta_{mm}}{2\eta}\right)\left(\sqrt{\frac{\pi}{\eta}}\right)^D \quad (11a)$$

$$\rho u_j = \left[\alpha_0 b_j + \frac{\alpha_j}{2\eta} + \frac{(D+2)a_j}{4\eta^2}\right]\left(\sqrt{\frac{\pi}{\eta}}\right)^D \quad (11b)$$

$$\frac{2D}{D_T + D_R}\left(\rho e + \frac{1}{2}\rho|\boldsymbol{u}|^2\right) = \frac{\rho D}{2\eta} + \sum_{k}^{D} \alpha_0 b_k^2 \left(\sqrt{\frac{\pi}{\eta}}\right)^D + \sum_{m}^{D} \frac{\beta_{mm}}{2\eta^2}\left(\sqrt{\frac{\pi}{\eta}}\right)^D \quad (11c)$$

$$\rho u_i u_j + p\delta_{ij} + P'_{ij} = \frac{\rho\delta_{ij}}{2\eta} + \alpha_0 b_i b_j \left(\sqrt{\frac{\pi}{\eta}}\right)^D + \frac{\beta_{ij} + \beta_{ji}}{4\eta^2}\left(\sqrt{\frac{\pi}{\eta}}\right)^D \quad (11d)$$

$$\left(\frac{D}{2} + \frac{D}{D_T + D_R}\right) p u_j + \frac{D}{D_T + D_R}\frac{1}{2}\rho|\boldsymbol{u}|^2 u_j = \left(1 + \frac{D}{2}\right)\frac{\rho u_j}{2\eta} + \frac{\alpha_0 b_j}{2}\sum_{k}^{D} b_k^2 \left(\sqrt{\frac{\pi}{\eta}}\right)^D + \frac{a_j}{8\eta^3}(D+2)\left(\sqrt{\frac{\pi}{\eta}}\right)^D \quad (11e)$$

From Eq. (11d), it is obvious that η can be determined by setting $p = \rho/2\eta$. Because the state equation for diatomic gas is given by $p = \rho\theta$, η is evaluated to be $\eta = 1/2\theta$. It now remains to solve P'_{ij} and determine $\alpha_0, \alpha_j, a_j, b_i$, and β_{mn} introduced in Eq. (10).

The coefficients $\alpha_0, \alpha_j, a_j, b_i$, and β_{mn} can be determined once P'_{ij} is known. The solution of P'_{ij} can be obtained by solving the divergence equation given in Eq. (9). One possible solution set for P'_{ij} can be written for an infinite domain $\mathbf{R}^D$ $(-\infty < x_i < \infty)$ [28] as

$$P'_{ij} = \frac{1}{2\pi}\int_{-\infty}^{\infty}\int_{-\infty}^{\infty} f(x'_i, x'_j)\,\ell_n \frac{1}{\sqrt{(x_i - x'_i)^2 + (x_j - x'_j)^2}}\,\mathrm{d}x'_i\,\mathrm{d}x'_j \quad \text{for } i \neq j \quad (12a)$$

$$P'_{ij} = -\int \sum_{k\neq i}^{D} \frac{\partial P'_{ik}}{\partial x_k}\,\mathrm{d}x_i \quad \text{for } i = j \quad (12b)$$

where

$$f(x'_i, x'_j) = \frac{D - (D_T + D_R)}{D_0(D_T + D_R)}\frac{\partial^2 \rho|\boldsymbol{u}|^2}{\partial x'_i \partial x'_j} \quad (12c)$$

$$\sum_{i=1}^{D} P'_{ii} = \frac{D - (D_T + D_R)}{D_T + D_R}\rho|\boldsymbol{u}|^2 \quad (12d)$$

with $D_0 = 1$ for 2-D flow and $D_0 = 3$ for 3-D flow. The solutions for both 2-D and 3-D cases can be easily written down from Eq. (12).

Assuming P'_{ij} is known, the coefficients of Eq. (10) can now be solved with the help of Eqs. (11a–11e) to give

$$\alpha_0 = \frac{\rho}{(\sqrt{2\pi\theta})^D} - \frac{D - (D_T + D_R)}{(D_T + D_R)\theta(\sqrt{2\pi\theta})^D}\frac{1}{2}\rho|\boldsymbol{u}|^2 \quad (13a)$$

$$\alpha_j = \frac{1}{\theta}\left[\frac{\rho u_j}{(\sqrt{2\pi\theta})^D} - \alpha_0 b_j - (D+2)\theta^2 a_j\right] \quad (13b)$$

$$a_j = \frac{1}{(D+2)\theta^3(\sqrt{2\pi\theta})^D}\left[u_j p\left\{\frac{D - (D_T + D_R)}{(D_T + D_R)}\right\} - \frac{b_j}{2}\rho|\boldsymbol{u}|^2 + \frac{D}{(D_T + D_R)}u_j\frac{1}{2}\rho|\boldsymbol{u}|^2\right] \quad (13c)$$

$$b_i = \frac{\pm u_i}{\sqrt{1 - [D - (D_T + D_R)/(D_T + D_R)\theta](1/2)|\boldsymbol{u}|^2}} \quad (13d)$$

$$\beta_{ij} = \frac{P'_{ij}}{2\theta^2(\sqrt{2\pi\theta})^D} \quad (13e)$$

These expressions have no undefined constants and all parameters either reduce to the BGK model identically or become zero for the monatomic gas case. For monatomic gas, $D_T = 3$, $D_R = 0$, and $P'_{ij} = 0$ for $i, j = 1, \ldots, D$. If the positive sign in Eq. (13d) is chosen, then $b_i = u_i$, $\alpha_0 = \rho/(\sqrt{2\pi\theta})^D$, $\alpha_i = a_i = 0$, and $\beta_{ij} = 0$ for $i, j = 1, \ldots, D$. It follows that f^{eq} as given in Eq. (10) reduces to a Maxwellian distribution and the original BGK model is exactly recovered.

III. Lattice f^{eq} and Velocity Lattice Model

A modified FDLBM is chosen as the numerical scheme to solve the BGK-type modeled BE. Therefore, it is necessary to write down the velocity space discretized form of Eq. (1). For a 2-D flow, the dimensionless lattice counterpart of Eq. (1) is

$$\frac{\partial f_\alpha}{\partial t} + \xi_\alpha \cdot \nabla_x f_\alpha = -\frac{1}{\tau Kn}(f_\alpha - f_\alpha^{\mathrm{eq}}) \quad (14)$$

where α is the index for the lattice velocity. A D2Q9 lattice model has been shown to be sufficient for accurate resolution of aeroacoustics problems [28]. If this formulation is to be generally applicable to aeroacoustics and shock capturing, then the same D2Q9 model should be tested. It has been shown that a finer lattice model, such as D2Q13, yields essentially identical results for aeroacoustics simulations [28]. Therefore, in later calculations, it will be demonstrated that results obtained from a D2Q9 and a D2Q13 model are essentially identical for shock-capturing simulations too. Consequently, the D2Q9 model is equally valid for aeroacoustics and

shock-capturing problems. Because the lattice f_α^{eq} for a D2Q13 model has already been given in Fu et al. [28], only the lattice f_α^{eq} for a D2Q9 model is given next. For such a model, the lattice velocity is distributed according to the following:

$$\xi_0 = 0, \qquad \alpha = 0 \tag{15a}$$

$$\xi_\alpha = \sigma\{\cos[\pi(\alpha-1)/4], \qquad \sin[\pi(\alpha-1)/4]\}, \qquad \alpha = 1,3,5,7 \tag{15b}$$

$$\xi_\alpha = \sqrt{2}\sigma\{\cos[\pi(\alpha-1)/4], \qquad \sin[\pi(\alpha-1)/4]\} \quad \alpha = 2,4,6,8 \tag{15c}$$

where σ is a parameter representing the magnitude of the velocity lattice and has to be determined.

Just as in the case of the continuous f^{eq}, the lattice f_α^{eq} also has to satisfy the Euler equations exactly if the assumption $M \ll 1$ is to be avoided. The method of Fu et al. [28] is free of this assumption. They accomplished this by postulating a polynomial series in $\boldsymbol{\xi}$ up to second order for f_α^{eq}. Each term in the series is weighted by coefficients that could be scalars, vectors, or tensors, depending on the nature of the term. Therefore, a polynomial series in the particle velocity ξ_α is assumed for the lattice f_α^{eq}, which to second order can be written as

$$f_\alpha^{\mathrm{eq}} = A_\alpha + \xi_{\alpha x} Ax_\alpha + \xi_{\alpha y} Ay_\alpha + \xi_{\alpha x}^2 Bxx_\alpha + \xi_{\alpha y}^2 Byy_\alpha + \xi_{\alpha x}\xi_{\alpha y} Bxy_\alpha \tag{16}$$

where the indices x and y are used to denote the x and y direction in a 2-D flow, and the coefficients A_α, Ax_α, Bxx_α, etc., can be scalars, vectors, or tensors. Here, x is the stream direction and y is normal to x. This proposed f_α^{eq}, which is different from conventional forms, in fact, attempts to include in Eq. (16) the particle–particle collision effect of the additional terms in Eq. (10). Its appropriateness for aeroacoustics simulations has already been demonstrated [28]. The objective of the present study is to further show that Eq. (16) is equally valid for FDLBM simulations of 1-D and 2-D compressible flows with shocks, contact discontinuities, slip lines, and expansion waves. Before proceeding to demonstrate this in subsequent sections, it could strengthen the present formulation by showing that the Euler equations can be recovered exactly from Eq. (16) using a D2Q9 lattice model without assuming $M \ll 1$.

The procedure for this derivation follows closely that detailed in Sec. II. Therefore, it is assumed that, for each α, f_α can be expanded as

$$f_\alpha = f_\alpha^{\mathrm{eq}} + Kn f_\alpha^{(1)} + Kn^2 f_\alpha^{(2)} + \mathcal{O}(Kn^3) \tag{17}$$

such that the following conditions are fulfilled. These conditions, in discrete form for 2-D flows in Cartesian coordinates, are obtained from Eqs. (4), (5), and (8), and are given by

$$\sum_{\alpha=0}^{N} f_\alpha^{\mathrm{eq}} = \rho \tag{18a}$$

$$\sum_{\alpha=0}^{N} f_\alpha^{\mathrm{eq}} \xi_{\alpha x} = \rho u \tag{18b}$$

$$\sum_{\alpha=0}^{N} f_\alpha^{\mathrm{eq}} \xi_{\alpha y} = \rho v \tag{18c}$$

$$\sum_{\alpha=0}^{N} f_\alpha^{\mathrm{eq}} (\xi_{\alpha x}^2 + \xi_{\alpha y}^2) = \frac{4}{D_T + D_R}\left(\rho e + \frac{1}{2}\rho|\boldsymbol{u}|^2\right) \tag{18d}$$

$$\sum_{\alpha=0}^{N} f_\alpha^{\mathrm{eq}} \xi_{\alpha x}^2 = \rho u^2 + p + P'_{xx} \tag{18e}$$

$$\sum_{\alpha=0}^{N} f_\alpha^{\mathrm{eq}} \xi_{\alpha y}^2 = \rho v^2 + p + P'_{yy} \tag{18f}$$

$$\sum_{\alpha=0}^{N} f_\alpha^{\mathrm{eq}} \xi_{\alpha x}\xi_{\alpha y} = \rho uv + P'_{xy} \tag{18g}$$

$$\sum_{\alpha=0}^{N} f_\alpha^{\mathrm{eq}} (\xi_{\alpha x}^2 + \xi_{\alpha y}^2)\xi_{\alpha x} = \frac{4u}{D_T + D_R}\left(\rho e + p + \frac{1}{2}\rho|\boldsymbol{u}|^2\right) \tag{18h}$$

$$\sum_{\alpha=0}^{N} f_\alpha^{\mathrm{eq}} (\xi_{\alpha x}^2 + \xi_{\alpha y}^2)\xi_{\alpha y} = \frac{4v}{D_T + D_R}\left(\rho e + p + \frac{1}{2}\rho|\boldsymbol{u}|^2\right) \tag{18i}$$

$$\sum_{\alpha=0}^{N} f_\alpha^{(n)} = 0 \quad \text{for } n \geq 1 \tag{18j}$$

$$\sum_{\alpha=0}^{N} f_\alpha^{(n)} \xi_{\alpha x} = 0 \quad \text{for } n \geq 1 \tag{18k}$$

$$\sum_{\alpha=0}^{N} f_\alpha^{(n)} \xi_{\alpha y} = 0 \quad \text{for } n \geq 1 \tag{18l}$$

$$\frac{D_T + D_R}{4} \sum_{\alpha=0}^{N} f_\alpha^{(n)} (\xi_{\alpha x}^2 + \xi_{\alpha y}^2) = 0 \quad \text{for } n \geq 1 \tag{18m}$$

Multiplying Eq. (14) with $(1, \xi_\alpha, |\xi_\alpha|^2\{D_T + D_R\}/4)^T$ and taking summation over α, after substituting Eq. (17) and using the constraints given in Eqs. (18), the following results are obtained for a 2-D flow (i.e., $D = 2$) in Cartesian coordinates

$$\frac{\partial \rho}{\partial t} + \frac{\partial \rho u}{\partial x} + \frac{\partial \rho v}{\partial y} + \mathcal{O}(Kn) = 0 \tag{19a}$$

$$\frac{\partial (\rho u)}{\partial t} + \frac{\partial}{\partial x}(\rho u^2 + p + P'_{xx}) + \frac{\partial}{\partial y}(\rho uv + P'_{xy}) + \mathcal{O}(Kn) = 0 \tag{19b}$$

$$\frac{\partial (\rho v)}{\partial t} + \frac{\partial}{\partial x}(\rho uv + P'_{xy}) + \frac{\partial}{\partial y}(\rho v^2 + p + P'_{yy}) + \mathcal{O}(Kn) = 0 \tag{19c}$$

$$\frac{\partial}{\partial t}\left(\rho e + \frac{1}{2}\rho|\boldsymbol{u}|^2\right) + \frac{\partial}{\partial x}\left[u\left(\rho e + p + \frac{1}{2}\rho|\boldsymbol{u}|^2\right)\right] + \frac{\partial}{\partial y}\left[v\left(\rho e + p + \frac{1}{2}\rho|\boldsymbol{u}|^2\right)\right] + \mathcal{O}(Kn) = 0 \tag{19d}$$

Once f_α^{eq} satisfies Eqs. (18), and P'_{xx}, P'_{yy}, and P'_{xy} satisfy the condition given in Eq. (9), the Euler equations, Eqs. (19a–19d), are exact subject to an error term of $\mathcal{O}(Kn)$. It should be pointed out that $Kn \ll 1$ is consistent with the assumption of a continuum fluid [28]. Therefore, for any given lattice model, once a suitable f_α^{eq} that satisfies Eqs. (18) is obtained, the Euler equations are recovered correctly. In other words, there is no M limitation on f_α^{eq} and the discrete modeled BE.

Of the nine equations in Eqs. (18), only eight are independent, because one is a duplicate of the kinetic energy equation. These equations are used to determine A_α, Ax_α, Bxx_α, etc. The equations have the elements of P'_{ij} as unknowns, which for a 2-D flow are reduced to P'_{xx}, P'_{xy}, and P'_{yy}; their values are given by solving Eqs. (12a–12d). If the coefficients having the same "energy shell" of the lattice velocities are assumed to be the same, the number of unknowns resulting from the coefficients A_α, Ax_α, Bxx_α, etc., are reduced to 13 in a D2Q9 lattice model. Because the number of constraints available for the determination of these coefficients is eight, there is a certain flexibility, and assumptions can be made to facilitate solution of the equations. As a first attempt, five coefficients out of the 13 are assumed zero. Details of this derivation are given in Fu et al. [28].

It should be noted that the solution thus obtained is not unique. However, there are no undefined constants, except σ, which can be determined as follows. From Eq. (18d) and making use of $p = \rho\theta$, the following bounds can be deduced for the particle velocity ξ_α, that is,

$$\min(|\xi_\alpha|^2)\sum_{\alpha=0}^{N} f_\alpha^{eq} \le \frac{4}{D_T + D_R}\left(\rho e + \frac{1}{2}\rho|\boldsymbol{u}|^2\right) \le \max(|\xi_\alpha|^2)\sum_{\alpha=0}^{N} f_\alpha^{eq} \tag{20}$$

Making use of Eq. (18a), Eq. (20) can be reduced to

$$\min(|\xi_\alpha|^2) \le 2\theta + \frac{2}{D_T + D_R}|\boldsymbol{u}|^2 \le \max(|\xi_\alpha|^2) \tag{21}$$

From Eq. (15b), the magnitude of σ is determined to be $\sigma^2 = |\xi_\alpha|^2$, or explicitly as

$$\sigma = |\xi_\alpha| = \left[\frac{2p_\infty}{\rho_\infty} + \frac{2}{D_T + D_R}(u_\infty^2 + v_\infty^2)\right]^{1/2} \tag{22}$$

for $\alpha = 1, 3, 5$, and 7 only. Thus formulated, numerical results are not subject to arbitrariness; however, their validity and extent has to be verified against known solutions.

IV. Finite Difference Lattice Boltzmann Model Simulation of Flows with Shocks

In aeroacoustics simulations, accuracy requirements necessitated the adoption of a numerical scheme consisting of a sixth-order finite difference method similar to that proposed by Lele [29] and a second-order Runge–Kutta time-marching scheme for the time-dependent term in the modeled BE. For compressible flow calculations with shocks, such a numerical scheme is not applicable; therefore, different numerical schemes suitable for capturing shocks need to be explored [35–37]. An appropriate time-marching numerical scheme would be one that uses a splitting method to resolve the inhomogeneous hyperbolic equation [Eq. (14)], whereas the split homogeneous hyperbolic equation is estimated using Harten's first-order upwind scheme [35]. In Harten's scheme, there is a parameter called the coefficient of artificial viscosity ε in the formulation; this is chosen as $\varepsilon = 0.01$ for 1-D flow and $\varepsilon = 0.05$ for 2-D flow. The grid spacing is set at $dx = 0.001$, whereas the time step is set at $dt = 0.00001$ for all 1-D calculations. For all 2-D cases attempted, $dx = dy = 0.0025$ and $dt = 0.0001$ are specified to expedite the numerical simulations. Later calculations show that these choices of dx, dy, and dt for 1-D and 2-D flows are quite sufficient to yield reliable results for the test cases investigated. Finally, at every time step, P'_{ij} has to be evaluated. For 1-D flows, because the problems are simulated in a 2-D domain, the top and bottom boundary conditions are specified by the periodic conditions, that is, the variables and their derivatives are the same at the top and bottom of the computational domain. As a result, $P'_{xy} = 0$ and this means that P'_{xx} can be evaluated from Eq. (12d). For 2-D flows, P'_{ij} can be obtained by solving Eqs. (12a–12d) or a Poisson equation derived from Eq. (9). A second-order Gauss–Seidel numerical scheme is used to solve the Poisson equation for all 2-D cases investigated.

In the present formulation, τ, Kn, and dt are related by $\tau Kn = dt$. Therefore, a choice of $dt = 0.00001$ or 0.0001 means that $\tau Kn = 0.00001$ or 0.0001 also. Because τ does not appear explicitly in the numerical scheme (it always appears as τKn), there is no loss of generality to assume $\tau = 1$ for all calculations, and the condition $Kn \ll 1$ still holds. This realization, together with the fact that σ can be evaluated exactly from Eq. (20), means that the choice of normalization is appropriate for the modeled BE. Further, calculations will show that the choice of τ is not important in the solution of the present BGK-type modeled BE. *It is this lack of arbitrariness that distinguishes the current approach from other BGK-type modeled BE.*

Calculations obtained from this modified FDLBM using Harten's first-order numerical scheme are validated against five known solutions of 1-D [9] and 2-D [38] Riemann problems. These known solutions consist of analytical results and numerical simulations obtained using Harten's first-order upwind scheme with flux vector splitting technique applied directly to the solution of the Euler equations. In the numerical simulations, $\varepsilon = 0.01$ is again assumed. Four of the five cases are compressible flows with shocks; only one case involves wave propagation in a compressible medium. Discussion of these results is given next.

V. Results for One-Dimensional Shocks

Three well-known 1-D test cases are selected; these are the Sod test, the Lax test, and the Roe test [9,35–37]. The first two cases have a shock, an expansion wave, and a contact discontinuity, whereas the third case has very strong rarefactions in the flow domain. The initial conditions of these three cases are given in Table 1. In this table, subscript L and R denote the inlet and outlet condition, respectively. The computational domain is bounded by $-0.5 \le x \le 0.5$. This means that there are 1000 grid points along the x direction. The outlet boundary conditions for p, u, ρ, and e are specified such that they are constant across the boundary.

The calculated distributions of p, u, ρ, and e for the Sod and Lax test case are shown in Figs. 1 and 2, respectively. The shock Mach number (which is defined as the speed of shock divided by the speed of sound ahead of the shock) of the Sod and Lax test case is 1.656 and 1.961, respectively. Their comparisons with analytical results will help establish the validity of the MEDF and the modified FDLBM. In these figures, three different solutions are shown: an exact solution denoted by a solid line, a numerical solution of the Euler equations designated by an open circle, and the present modified FDLBM solution denoted by an x. It can be seen that all three solutions are essentially identical except around the knee where drastic changes occur for p, u, ρ, and e. This means that the expansion waves are replicated correctly, the shock is capture precisely, and the contact discontinuity is calculated accurately for these two cases. The present solutions and those obtained from numerically solving the Euler equations are identical and are essentially the same as those reported

Table 1 Initial condition for the three 1-D test cases

Test cases	$-0.5 < x < 0$			$0 < x < 0.5$		
	ρ_L	u_L	p_L	ρ_R	u_R	p_R
Sod [9,36]	1	0	1	0.125	0	0.1
Lax [9,35]	0.445	0.698	3.528	0.5	0	0.571
Roe [9,37]	1	−1	1.8	1	1	1.8

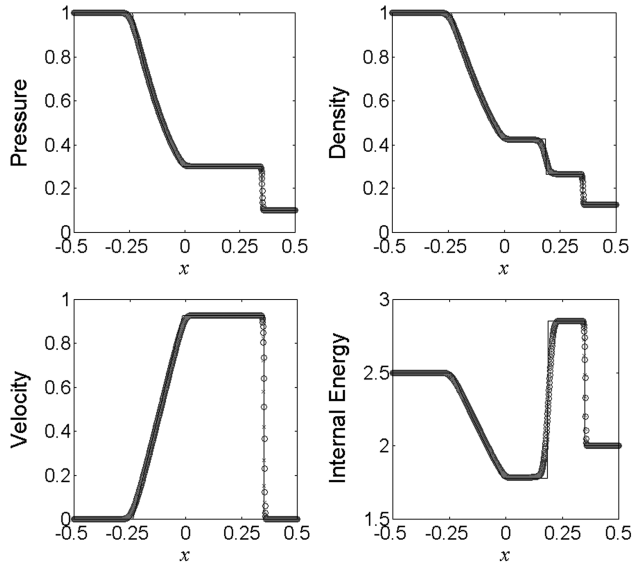

Fig. 1 Sod test case: solid line, exact solution; symbol x is the modified LBM simulation; and symbol o is the Euler equation solved using first-order upwind scheme of Harten [35] with flux vector splitting for p, ρ, u, and e at time $t = 0.2$.

in Shi et al. [9]; however, they are deduced without any arbitrary constants in the modified FDLBM using a D2Q9 lattice model.

The effects of grid size and the number of velocity lattices are investigated next. Only the Sod test case is used for this investigation. The finer grid results have already been obtained and they are shown in Fig. 1. A calculation using a coarser grid with $dx = 0.01$ (all other settings are the same as those listed under the Sod test case) and the same D2Q9 lattice model was carried out. The results, together with those obtained from $dx = 0.001$, are plotted in Fig. 3a for comparison. Another calculation was carried out using a finer lattice model, namely, a D2Q13 model. The lattice distribution for the D2Q13 model has been given in Fu et al. [28] and, therefore, will not be repeated here. These results, together with those obtained using a D2Q9 model, are plotted in Fig. 3b for comparison.

The modified FDLBM is only a first-order scheme; therefore, the results are less than satisfactory in Fig. 3a. Refining the grid leads to tremendous improvements in the simulated results (Figs. 1 and 3b).

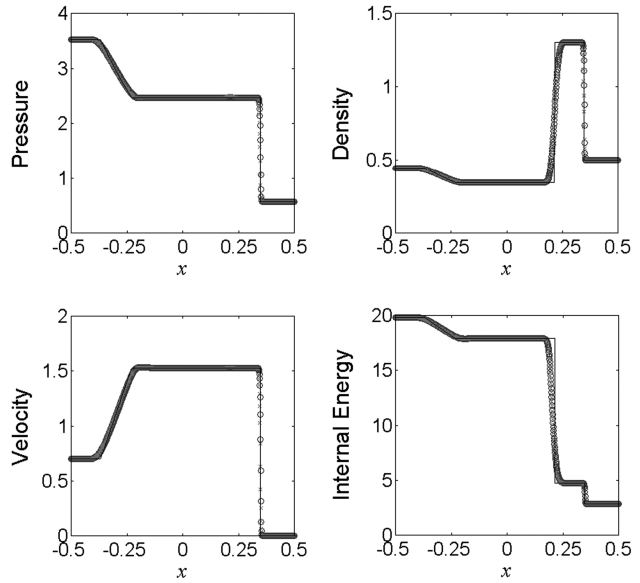

Fig. 2 Lax test case: solid line, exact solution; symbol x is the modified LBM simulation; and symbol o is the Euler equation solved using first-order upwind scheme of Harten [35] with flux vector splitting for p, ρ, u, and e at time $t = 0.14$.

This refinement improves the simulated results for the D2Q9 and D2Q13 models equally, because there is essentially no difference between their calculations (Fig. 3b). This shows that a D2Q9 model is just as appropriate as a D2Q13 model. The same conclusion has also been drawn by Fu et al. [28] in their simulations of aeroacoustics problems. Therefore, these results show that a D2Q9 model is good enough for the recovery of the Euler equations to $\mathcal{O}(Kn)$, at least for the shock-capturing problems presented. The shock structure observed in Figs. 1 and 3 is due to numerical smearing and is present irrespective of whether the discrete modeled BE is solved or whether the Euler equations are solved directly using Harten's first-order scheme (Figs. 1 and 2).

The results of the Roe test case are shown in Fig. 4. Again, the same symbols are used to denote the solutions of the theoretical analysis, the numerically solved Euler equations, and the modified FDLBM. All three solutions are essentially identical except near the knee where drastic changes of p, u, ρ, and e are observed. However, the present solutions and those of the Euler equations are identical. Both of these solutions show an error in the middle of the ρ and e profiles compared to the exact solutions. It is not clear why these errors occur. They also appear in the numerical simulation study of Shi et al. [9], where a TVD scheme was adopted with either a minmod function or a second-order corrector as the flux limiter. The TVD treatment is not necessary for the present simulation, thus lending further evidence to the robustness of the modified FDLBM to correctly resolve velocity discontinuity in a compressible flow.

The ability of the modified FDLBM to resolve shocks, expansion and compression waves, and contact discontinuity in 1-D compressible flows has been established. This success can be

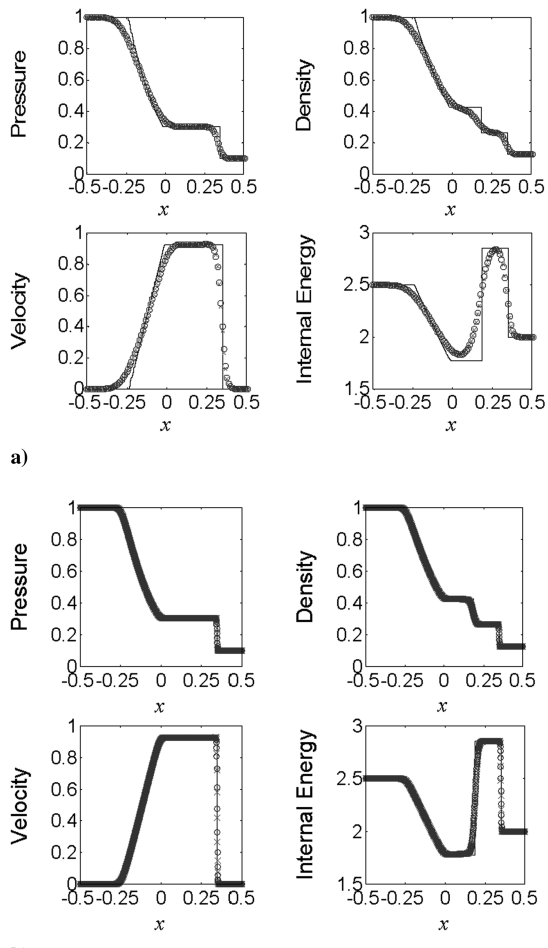

Fig. 3 Sod test case: solid line, exact solution; symbol x is the modified FDLBM simulation with a D2Q9 model; and symbol o is the modified FDLBM simulation with a D2Q13 model at time $t = 0.2$ and a) $dx = dy = 0.01$, b) $dx = dy = 0.001$.

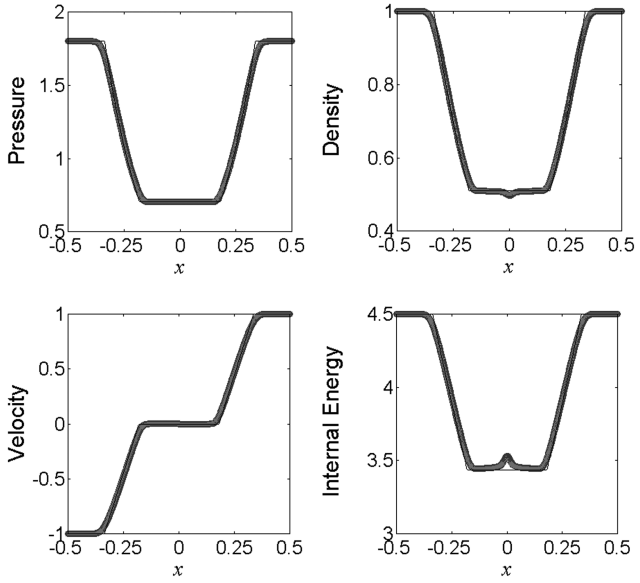

Fig. 4 Roe test case: solid line, exact solution; symbol x is the modified LBM simulation; and symbol o is the Euler equation solved using the first-order upwind scheme of Harten [35] with flux vector splitting for p, ρ, u, and e at time $t = 0.13$.

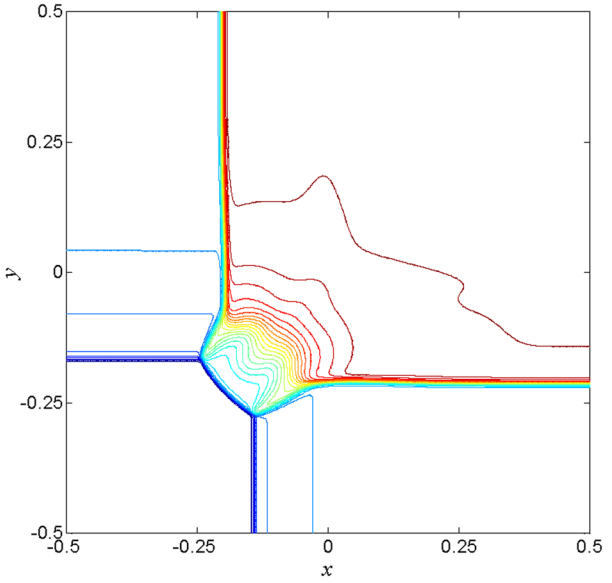

Fig. 5 Two-dimensional test case: density contour of configuration 3 of the 2-D Riemann problem [38] calculated by the modified FDLBM at $t = 0.3$ (there are 28 evenly distributed contour lines between 0.1371 and 1.5011). The maximum is the outermost contour in quadrant 1 and the minimum is the outermost contour in quadrant 3.

attributed to the MEDF f^{eq}, where, besides the conventional Maxwellian term, three more terms to model particle–particle collisions are also present. The additional terms are directly responsible for the correct capturing of the shocks in the Sod and Lax test cases compared with frequently adopted forms of continuous or lattice f^{eq} used by other researchers. These results and those on aeroacoustics simulations [28] suggest that Eq. (10) and its lattice counterpart [Eq. (16)] are good alternatives to the Euler equations for aeroacoustics and inviscid compressible flow simulations.

The errors between the FDLBM simulation and the solution of the Euler equations of a macroscopic variable $\boldsymbol{b}$ are expressed in terms of the integral norm L_q and its maximum, that is,

$$\|L_q(\boldsymbol{b})\| = \left[\frac{1}{N}\sum_{j=1}^{N}|\boldsymbol{b}_{\text{LBM},j} - \boldsymbol{b}_{\text{EULER},j}|^q\right]^{\frac{1}{q}} \tag{23a}$$

Table 2 Error norms for the three 1-D cases

Error norms	L_∞	L_1	L_2
	Sod test case		
p	0.0789	0.0018	0.0057
u	0.3708	0.0039	0.0242
ρ	0.0531	0.0018	0.0043
	Lax test case		
p	0.6401	0.0080	0.0445
u	0.4743	0.0053	0.0320
ρ	0.2801	0.0045	0.0220
	Roe test case		
p	0.0212	0.0047	0.0080
u	0.0189	0.0042	0.0071
ρ	0.0096	0.0022	0.0036

$$\|L_\infty(\boldsymbol{b})\| = \max_j|\boldsymbol{b}_{\text{LBM},j} - \boldsymbol{b}_{\text{EULER},j}| \tag{23b}$$

Thus defined, the calculated error norms of p, u, and ρ are tabulated in Table 2 for the three 1-D cases. It can be seen that the calculated L_q are small; in general, they are on the order of 10^{-2} or smaller. The L_∞ is much larger because of the disagreement around the knees of the p, u, and ρ distributions. This suggests that the modified FDLBM using Eq. (16) is a viable alternative to the Euler equations in capturing 1-D shocks.

VI. Results for Two-Dimensional Shocks

Having demonstrated the ability of the modified FDLBM to resolve shocks up to $M = 1.961$ for 1-D compressible flows, the next step is to verify its ability to resolve 2-D flows with shocks. The two cases selected are the 2-D Riemann problems treated by Lax and Liu [38]. The 2-D domain is divided into four quadrants and the flow conditions specified in each quadrant are assumed to be constant initially. The constants in the four quadrants are selected so that only a 1-D shock, a 1-D expansion wave, or a slip line appears at each interface. Only two different configurations are attempted: these are configuration 3 and configuration 4 of Lax and Liu [38]. The initial conditions for these two cases are listed in Table 3. The computational domain is again selected to be $-0.5 \le x \le 0.5$. Since $dx = dy = 0.0025$, the number of grid points along the x and y direction is 400×400. This coarser grid is used because of limitations on computational resources at Hong Kong Polytechnic University. It is recognized that this grid might not be able to reproduce the finer details of the flowfield, however, it would allow the gross features of the flow in the domain to be replicated. Further, any bounceback from the boundaries would be visible even in this coarse grid, thus revealing the inadequacy of the boundary

Table 3 Initial condition for the two 2-D test cases; numbering of the four quadrants is counterclockwise, beginning with 1 at the top right-hand quadrant

Configuration	Quadrant condition			
3	$p_2 = 0.3\ u_2 = 1.206$	$\rho_2 = 0.5323\ v_2 = 0$	$p_1 = 1.5\ u_1 = 0$	$\rho_1 = 1.5\ v_1 = 0$
	$p_3 = 0.029\ u_3 = 1.206$	$\rho_3 = 0.138\ v_3 = 1.206$	$p_4 = 0.3\ u_4 = 0$	$\rho_4 = 0.5323\ v_4 = 1.206$
Configuration	Quadrant condition			
4	$p_2 = 0.35\ u_2 = 0.8939$	$\rho_2 = 0.5065\ v_2 = 0$	$p_1 = 1.1\ u_1 = 0$	$\rho_1 = 1.1\ v_1 = 0$
	$p_3 = 1.1\ u_3 = 0.8939$	$\rho_3 = 1.1\ v_3 = 0.8939$	$p_4 = 0.35\ u_4 = 0$	$\rho_4 = 0.5065\ v_4 = 0.8939$

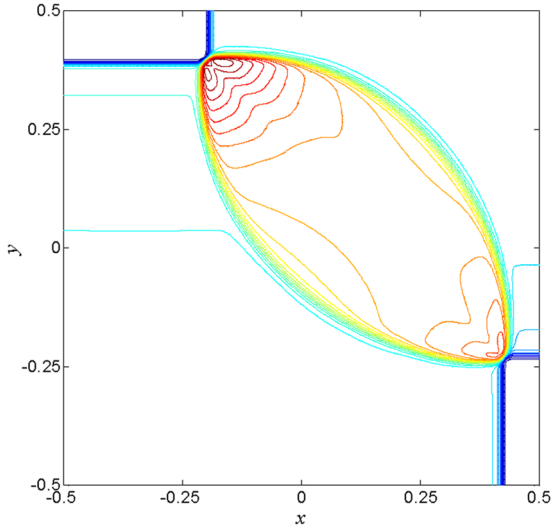

Fig. 6 Two-dimensional test case: density contour of configuration 4 of the 2-D Riemann problem [38] calculated by the modified LBM at $t = 0.25$ (there are 28 evenly distributed evenly distributed contour lines between 0.5064 and 2.1040). The maximum is the innermost contours within the ellipse and the minimum is the outermost contours in quadrants 2 and 4.

conditions proposed for f and P'_{ij}. The boundary conditions for p, u, ρ, and e are again specified such that they are continuous across all boundaries.

The 2-D Riemann problems (configurations 3 and 4 of Lax and Liu [38]) chosen have the characteristics that each planar wave at an interface connecting two neighboring constant states consists of a 1-D expansion wave, a 1-D shock wave, or a slip line. Correct resolution of these characteristics is further evidence of the ability of the modified FDLBM. As before, there is no need to adjust any arbitrary constants because there are none to be adjusted. All constants that appear in the modified FDLBM are obtained from the derivation of the MEDF f^{eq} and its lattice counterpart. The results for configurations 3 and 4 are shown in Figs. 5 and 6, respectively. Overall, the trend is essentially identical to those shown in Lax and Liu [38], and the solutions are clean without any bounceback from the boundaries. The difference is in the details of the inner structure. Because the same grid size as that adopted in Lax and Liu [38] is used in the present simulation, the difference could be attributed to the use of a less accurate numerical scheme: Harten's first-order scheme versus the positivity scheme of Lax and Liu [38], which is of second-order accuracy.

These 2-D results, no doubt demonstrate the ability of Eqs. (10) and (16) to replicate 2-D compressible flows with shocks, slip lines, and expansion waves. In other words, the additional terms in Eq. (16) are appropriate in their modeling of particle collisions and their momentum and energy exchange resulting from these collisions. Apparently, a correct modeling of this behavior is essential to the proper replication of the effect resulting from the interaction between shocks, slip lines, and expansion waves. Other researchers attempted to remedy the inadequacy of the conventional f^{eq} by adjusting τ or some arbitrary parameters. Such treatments are not necessary in the present approach.

The plots of P'_{ij} behavior for configurations 3 and 4 are shown in Figs. 7 and 8, respectively. In general, their behavior is very similar to those shown in Figs. 5 and 6 for configurations 3 and 4, respectively; again the solutions are free of disturbances resulting from bounceback at the boundaries. These plots show that P'_{ij} are by no means small; their magnitudes are on the order of one, as indicated by their maximum and minimum values. They contribute to the calculations of p, u, and ρ through Eqs. (18e–18g); their neglect could affect the errors in the prediction of the shock, expansion wave, and slip line. Therefore, they play a crucial role in the correct recovery of the Euler equations from the discretized modeled BE. All these results show that the boundary conditions invoked for f and P'_{ij} are appropriate, and the modified FDLBM proves to be a viable alternative to solving the Euler equations for compressible flows with shocks.

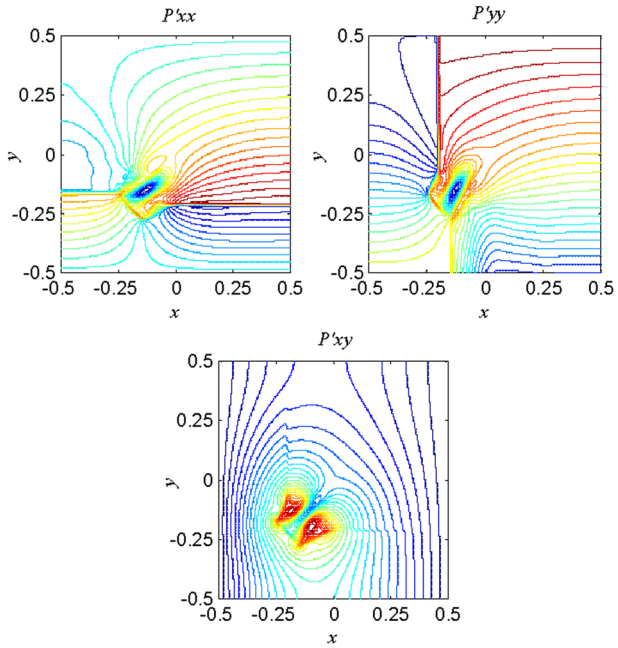

Fig. 7 The P'_{ij} behavior for configuration 3 (there are 28 evenly distributed contour lines) at $t = 0.3$. The (maximum, minimum) values of P'_{xx}, P'_{yy}, and P'_{xy} are (0.25787, −0.16919), (−0.00078, −0.48353), and (0.34463, 0), respectively. For P'_{xx}, the maximum occurs in the upper part of quadrant 4, whereas the minimum occurs near the eye of the vortex in quadrant 3; for P'_{yy}, the maximum occurs in the lower part of quadrant 1, whereas the maximum occurs near the eye of the vortex in quadrant 3; for P'_{xy}, the maximum occurs near the eye of the vortices in quadrant 3, whereas the minimum occurs at the outermost contours running through quadrants 1 and 4, and 2 and 3.

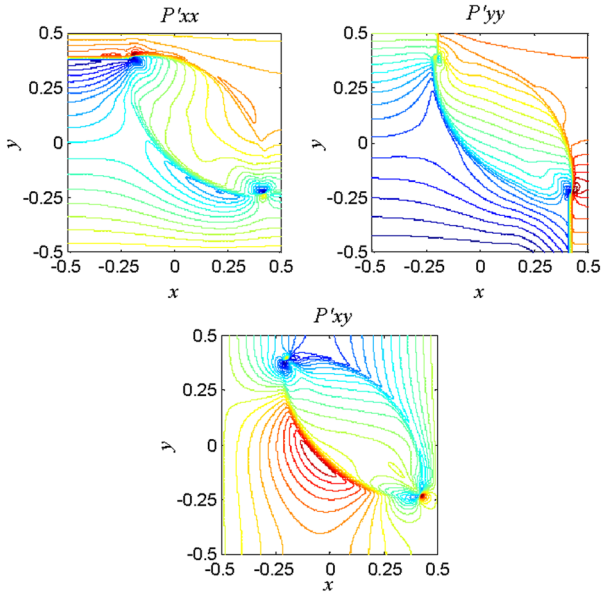

Fig. 8 The P'_{ij} behavior for configuration 4 (there are 28 evenly distributed contour lines) at $t = 0.25$. The (maximum, minimum) values of P'_{xx}, P'_{yy}, and P'_{xy} are (0.29343, −0.53522), (0.23725, −0.90106), and (0.21935, −0.30326), respectively. For P'_{xx}, the maximum occurs near the upper part of quadrants 1 and 2, whereas the minimum occurs near the eye of the two vortices; for P'_{yy}, the maximum occurs in the right side of quadrants 1 and 4, whereas the minimum occurs near the bottom of quadrant 3; for P'_{xy}, the maximum occurs near the edge of the shock in quadrants 2 and 3, whereas the minimum occurs near the eye in the vortex located in quadrant 1.

VII. Conclusions

A modified FDLBM is formulated based on an MEDF f^{eq} that allows the Euler equations to be recovered exactly using either the continuous or the discretized form of f^{eq}. To accomplish this requirement, an additional equation for a second-order tensor P'_{ij} needs to be solved. In general, the equation for P'_{ij} is a Poisson equation and the solution for an infinite domain can be obtained analytically. The numerical simulation solves the lattice f^{eq} by adopting a D2Q9 velocity lattice model. Thus derived, the modified FDLBM has no arbitrary constants. The modified FDLBM with a D2Q9 velocity lattice is tested against 1-D and 2-D Riemann problems with shocks, expansion waves, and contact discontinuity.

The simulated results are validated against analytical solutions and numerical solutions obtained by solving the Euler equations using the first-order upwind scheme of Harten [35]. For 1-D Riemann problems, all three solutions are essentially identical except near the knee where drastic changes of p, u, ρ, and e occur. Both numerical solutions show the same behavior; therefore, it is not a drawback of the modified FDLBM scheme. Rather, it is a consequence of numerical smearing. For 2-D Riemann problems, the modified FDLBM solutions thus obtained are in general agreement with those given by Lax and Liu [38]. The difference is in the finer details of the wave structure bounded by the shocks and slip lines. This could be attributed to the first-order numerical scheme used in the present calculations compared to a second-order scheme used by Lax and Liu [38]. The present study, therefore, demonstrates the ability of the MEDF f^{eq} to resolve compressible flows with shocks, contact discontinuity, and expansion waves with accuracy equal to that given by solving the Euler equations directly using the same first-order numerical scheme.

Acknowledgments

Support from the Research Grants Council of the Government of the Hong Kong Special Administrative Region given under grant numbers PolyU1/02C, PolyU5303/03E, and PolyU5272/04E, and from the Hong Kong Polytechnic University given under grant numbers A-PA2U and A-PA5U is gratefully acknowledged.

References

[1] Mott-Smith, H. M., "The Solution of the Boltzmann Equation for a Shock Wave," *Physical Review*, Vol. 82, No. 6, 1951, pp. 885–892. doi:10.1103/PhysRev.82.885

[2] Chapman, S., and Cowling, T. G., *The Mathematical Theory of Non-Uniform Gases*, Cambridge Univ. Press, Cambridge, England, U.K., 1939.

[3] Salwen, H., Grousch, C. E., and Ziering, S., "Extension of the Mott-Smith Method for a One-Dimensional Shock Wave," *Physics of Fluids*, Vol. 7, No. 2, 1964, pp. 180–189. doi:10.1063/1.1711131

[4] Bhatnagar, P. L., Gross, E. P., and Krook, M., "A Model for Collision Processes in Gases, I: Small Amplitude Processes in Charged and Neutral One-Component Systems," *Physical Review*, Vol. 94, No. 3, 1954, pp. 511–525. doi:10.1103/PhysRev.94.511

[5] Li, X. M., Leung, R. C. K., and So, R. M. C., "One-Step Aeroacoustics Simulation Using Lattice Boltzmann Method," *AIAA Journal*, Vol. 44, No. 1, 2006, pp. 78–89. doi:10.2514/1.15993

[6] Alexander, F. J., Chen, S., and Sterling, J. D., "Lattice Boltzmann Thermohydrodynamics," *Physical Review E: Statistical Physics, Plasmas, Fluids, and Related Interdisciplinary Topics*, Vol. 47, No. 4, 1993, pp. R2249–R2252. doi:10.1103/PhysRevE.47.R2249

[7] Chen, Y., Ohashi, H., and Akiyama, M., "Thermal Lattice Bhatnagar-Gross-Krook Model Without Nonlinear Deviations in Macrodynamic Equations," *Physical Review E: Statistical Physics, Plasmas, Fluids, and Related Interdisciplinary Topics*, Vol. 50, No. 4, 1994, pp. 2776–2783. doi:10.1103/PhysRevE.50.2776

[8] Yan, G., Chen, Y., and Hu, S., "Simple Lattice Boltzmann Model for Simulating Flows with Shock Wave," *Physical Review E: Statistical Physics, Plasmas, Fluids, and Related Interdisciplinary Topics*, Vol. 59, No. 1, 1999, pp. 454–459. doi:10.1103/PhysRevE.59.454

[9] Shi, W., Shyy, W., and Mei, R., "Finite-Difference-Based Lattice Boltzmann Method for Inviscid Compressible Flows," *Numerical Heat Transfer, Part B: Fundamentals*, Vol. 40, No. 1, 2001, pp. 1–21. doi:10.1080/104077901300233578

[10] Kataoka, T., and Tsutahara, M., "Lattice Boltzmann Model for the Compressible Euler Equations," *Physical Review E: Statistical Physics, Plasmas, Fluids, and Related Interdisciplinary Topics*, Vol. 69, No. 5, 2004, p. 056702. doi:10.1103/PhysRevE.69.056702

[11] Sun, C., "Lattice-Boltzmann Models for High Speed Flow," *Physical Review E: Statistical Physics, Plasmas, Fluids, and Related Interdisciplinary Topics*, Vol. 58, No. 6, 1998, pp. 7283–7287. doi:10.1103/PhysRevE.58.7283

[12] Sun, C., "Simulations of Compressible Flows with Strong Shocks by an Adaptive Lattice Boltzmann Model," *Journal of Computational Physics*, Vol. 161, No. 1, 2000, pp. 70–84. doi:10.1006/jcph.2000.6487

[13] Sun, C., and Hsu, A. T., "Three-Dimensional Lattice Boltzmann Model for Compressible Flows," *Physical Review E: Statistical Physics, Plasmas, Fluids, and Related Interdisciplinary Topics*, Vol. 68, No. 1, 2003, pp. 016303.1–016303.14. doi:10.1103/PhysRevE.68.016303

[14] Feng, S. D., Dong, P., Tsutahara, M., and Takada, N., "Simulation of Shockwave Propagation with a Thermal Lattice Boltzmann Model," *International Journal for Numerical Methods in Fluids*, Vol. 41, No. 11, 2003, pp. 1137–1146. doi:10.1002/fld.481

[15] Tsutahara, M., Kataoka, T., Takada, N., Kang, H. K., and Kurita, M., "Simulations of Compressible Flows by Using the Lattice Boltzmann and the Finite Difference Lattice Boltzmann Methods," *Computational Fluid Dynamics Journal*, Vol. 11, No. 1, 2002, pp. 486–493.

[16] Kataoka, T., and Tsutahara, M., "Lattice Boltzmann Model for the Compressible Navier–sStokes Equations with Flexible Specific-Heat Ratio," *Physical Review E: Statistical Physics, Plasmas, Fluids, and Related Interdisciplinary Topics*, Vol. 69, No. 3, 2004, pp. 035701. doi:10.1103/PhysRevE.69.035701

[17] Qian, Y. H., and Orszag, S. A., "Lattice BGK Models for the Navier–Stokes Equation: Nonlinear Deviation in Compressible Regimes," *Europhysics Letters*, Vol. 21, No. 3, 1993, pp. 255–259. doi:10.1209/0295-5075/21/3/001

[18] Yang, J. Y., and Huang, J. C., "Rarefied Flow Computations Using Nonlinear Model Boltzmann Equations," *Journal of Computational Physics*, Vol. 120, No. 2, 1995, pp. 323–339. doi:10.1006/jcph.1995.1168

[19] Li, Z. H., and Zhang, H. X., "Study on Gas Kinetic Unified Algorithm for Flows from Rarefied Transition to Continuum," *Journal of Computational Physics*, Vol. 193, No. 2, 2004, pp. 708–738. doi:10.1016/j.jcp.2003.08.022

[20] Chu, C. K., "Kinetic-Theoretic Description of the Formation of a Shock Wave," *Physics of Fluids*, Vol. 8, No. 1, 1965, pp. 12–22. doi:10.1063/1.1761077

[21] MacCormack, R. W., "The Effect of Viscosity in Hypervelocity Impact Cratering," AIAA Paper No. 69-354, 1969.

[22] Xu, K., "A New Class of Gas-Kinetic Relaxation Schemes for the Compressible Euler Equations," *Journal of Statistical Physics*, Vol. 81, Nos. 1–2, 1995, pp. 147–164. doi:10.1007/BF02179973

[23] Chit, O. J., Omar, A. A., Asrar, W., and Hamdan, M. M., "Implicit Gas-Kinetic Bhatnagar-Gross-Krook Scheme for Compressible Flows," *AIAA Journal*, Vol. 42, No. 7, 2004, pp. 1293–1301. doi:10.2514/1.2171

[24] Xu, K., "A Gas-Kinetic BGK Scheme for the Navier–Stokes Equations and Its Connection with Artificial Dissipation and Godunov Method," *Journal of Computational Physics*, Vol. 171, No. 1, 2001, pp. 289–335. doi:10.1006/jcph.2001.6790

[25] Xu, K., and He, X., "Lattice Boltzmann Method and Gas-Kinetic BGK Scheme in the Low-Mach Number Viscous Flow Simulations," *Journal of Computational Physics*, Vol. 190, No. 1, 2003, pp. 100–117. doi:10.1016/S0021-9991(03)00255-9

[26] Xu, K., and Tang, L., "Nonequilibrium Bhatnagar-Gross-Krook Model for Nitrogen Shock Structure," *Physics of Fluids*, Vol. 16, No. 10, 2004, pp. 3824–3827. doi:10.1063/1.1783372

[27] Xu, K., and Josyula, E., "Gas-Kinetic Scheme for Rarefied Flow Simulation," *Mathematics and Computers in Simulation*, Vol. 72, Nos. 2–6, 2006, pp. 253–256. doi:10.1016/j.matcom.2006.05.028

[28] Fu, S. C., So, R. M. C., and Leung, R. C. K., "Modeled Boltzmann Equation and Its Application to Direct Aeroacoustics Simulation," *AIAA Journal*, Vol. 46, No. 7, 2008, pp. 1651–1662. doi:10.2514/1.33250

[29] Lele, S. K., "Direct Numerical Simulations of Compressible Turbulent Flows: Fundamentals and Applications," *Transition, Turbulence and Combustion Modeling*, Chap. 7, Kluwer Academic, London, 1998, pp. 424–429, 436–443.

[30] Wolf-Gladrow, D. A., *Lattice-Gas Cellular Automata and Lattice Boltzmann Models, An Introduction*, Chap. 5, Springer–Verlag, New York, 2000.

[31] Chen, S., and Doolen, G. D., "Lattice Boltzmann Method for Fluid Flows," *Annual Review of Fluid Mechanics*, Vol. 30, Jan. 1998, pp. 329–364. doi:10.1146/annurev.fluid.30.1.329

[32] Wang Chang, C. S., Uhlenbeck, G. E., and deBoer, J., *Studies in Statistical Mechanics*, Vol. 2, edited by J. deBoer, and G. E. Uhlenbeck, Wiley, New York, 1964.

[33] Harris, S., *An Introduction to the Theory of the Boltzmann Equation*, Dover, New York, 1999, Chaps. 1–4.

[34] Morse, T. F., "Kinetic Model for Gases with Internal Degrees of Freedom," *Physics of Fluids*, Vol. 7, No. 2, 1964, pp. 159–169. doi:10.1063/1.1711128

[35] Harten, A., "High Resolution Schemes for Hyperbolic Conservation Laws," *Journal of Computational Physics*, Vol. 49, No. 3, 1983, pp. 357–393. doi:10.1016/0021-9991(83)90136-5

[36] Sod, G. A., "A Survey of Several Finite Difference Methods for Systems of Nonlinear Hyperbolic Conservation Laws," *Journal of Computational Physics*, Vol. 27, No. 1, 1978, pp. 1–31. doi:10.1016/0021-9991(78)90023-2

[37] Einfeldt, B., Munz, C. D., Roe, P. L., and Sjögreen, B., "On Godunov-Type Methods near Low Densities," *Journal of Computational Physics*, Vol. 92, No. 2, 1991, pp. 273–295. doi:10.1016/0021-9991(91)90211-3

[38] Lax, P. D., and Liu, X. D., "Solution of Two-Dimensional Riemann Problems of Gas Dynamics by Positive Schemes," *SIAM Journal on Scientific Computing*, Vol. 19, No. 2, 1998, pp. 319–340. doi:10.1137/S1064827595291819

K. Powell
Associate Editor